Volume Strain Measurements on $CaCO_3$/Polypropylene Particulate Composites: The Effect of Particle Size

A. Lazzeri,[1] Y. S. Thio,[2] R. E. Cohen[2]

[1]*Department of Chemical Engineering, Industrial Chemistry and Materials Science, University of Pisa, Via Diotisalvi 2, 56126 Pisa, Italy*
[2]*Department of Chemical Engineering, Massachusetts Institute of Technology, 77 Massachusetts Avenue, Cambridge, Massachusetts 02139-4307*

Received 2 December 2002; accepted 12 May 2003

ABSTRACT: The use of rigid fillers to toughen polymers has received considerable attention in recent years. The role of the rigid particle here is that of debonding, at some stage, from the matrix, thus triggering dilatational processes similar to those observed in rubber-toughened polymers. The role of particle size in these rigid filled composites has not been studied in great detail. In this work, volume strain measurements were carried out on a series of particulate composites based on polypropylene filled with calcium carbonate (CC) particles with average diameters of 0.07, 0.7, and 3.5 μm and filler volume fractions ranging from 0.05 to 0.30. The experimental results have shown a strong particle size effect. A model is proposed to take this effect into account, based upon the formation of an immobilized layer of polymer on the surface of the filler particles. The experimental results are consistent with a surface layer of 15–25 nm. The results are discussed in relation to the fracture behavior of these composites reported earlier. © 2003 Wiley Periodicals, Inc. J Appl Polym Sci 91: 925–935, 2004

Key words: poly(propylene) (PP), composites, fillers, mechanical properties

INTRODUCTION

The toughness of commodity plastics at extreme conditions such as impact loading and low temperatures can be improved by incorporation of particulate fillers. Recently, Lazzeri and Bucknall have elucidated a mechanism for polymer toughening using rubber particles.[1–3] They showed that these particles can facilitate the development of microvoids and activate dilatational yielding in the deformed zone close to the fracture surface. The use of rigid fillers to toughen polymers has also received considerable attention in recent years. For example, toughening of isotactic polypropylene (iPP) using calcium carbonate ($CaCO_3$) has been reported.[4–7] Similar to the requirement of void creation via cavitation in the rubber-toughening mechanism, it is generally agreed that for toughening to occur in rigid filler systems, the particles must debond from the matrix, creating voids around the particles and allowing the interparticle ligaments to deform plastically.[8–10] The voids reduce the macroscopic plastic resistance of the material, and thereby potentially increase the fracture strain and the overall toughness. Ideally, the voids are likely to not form immediately upon application of stress as this may reduce the elastic modulus. The criterion for particle–matrix debonding can be as simple as a critical stress such as shown in the case of $CaCO_3$ filled Nylon-6,[11] where the debonding stress is roughly determined by the residual thermal stresses due to processing. In most systems, debonding is a distributed process, occurring over a range of stresses and strains. Several studies have observed the onset of debonding using mechanical property measurements[9] and acoustic methods.[12-13]

Although there are hundreds of articles on the topic of inorganic particle-filled iPP, only a few of these explicitly address the effect of particle size. Furthermore, most of the latter category shows the effect of particle size in the context of figure-of-merit property elucidation. Here, we focus on the role of particle size on mechanistic issues involved in the deformation and toughness of iPP compounds containing rigid fillers.

The study presented here used tensile dilatometry to observe the debonding process and the evolution of volume with increasing strain. This method of measuring volume change during uniaxial tensile test has been used to study toughening mechanisms in rubber-filled polymers.[14] If the rubber particles cavitate during deformation, the volume of the cavities will increase with strain in addition to the volume change of the matrix itself. Similarly, in the rigid filler case, the

Correspondence to: A. Lazzeri. (a.lazzeri@ing.unipi.it).
Contract grant sponsor: NSF MRSEC program through the Center of Materials Science and Engineering at MIT (to Y.S.T. and R.E.C.); contract grant number: DMR-98-08941.
Contract grant sponsor: the Defense University Research Initiative on NanoTechnology (DURINT) program.

Journal of Applied Polymer Science, Vol. 91, 925–935 (2004)

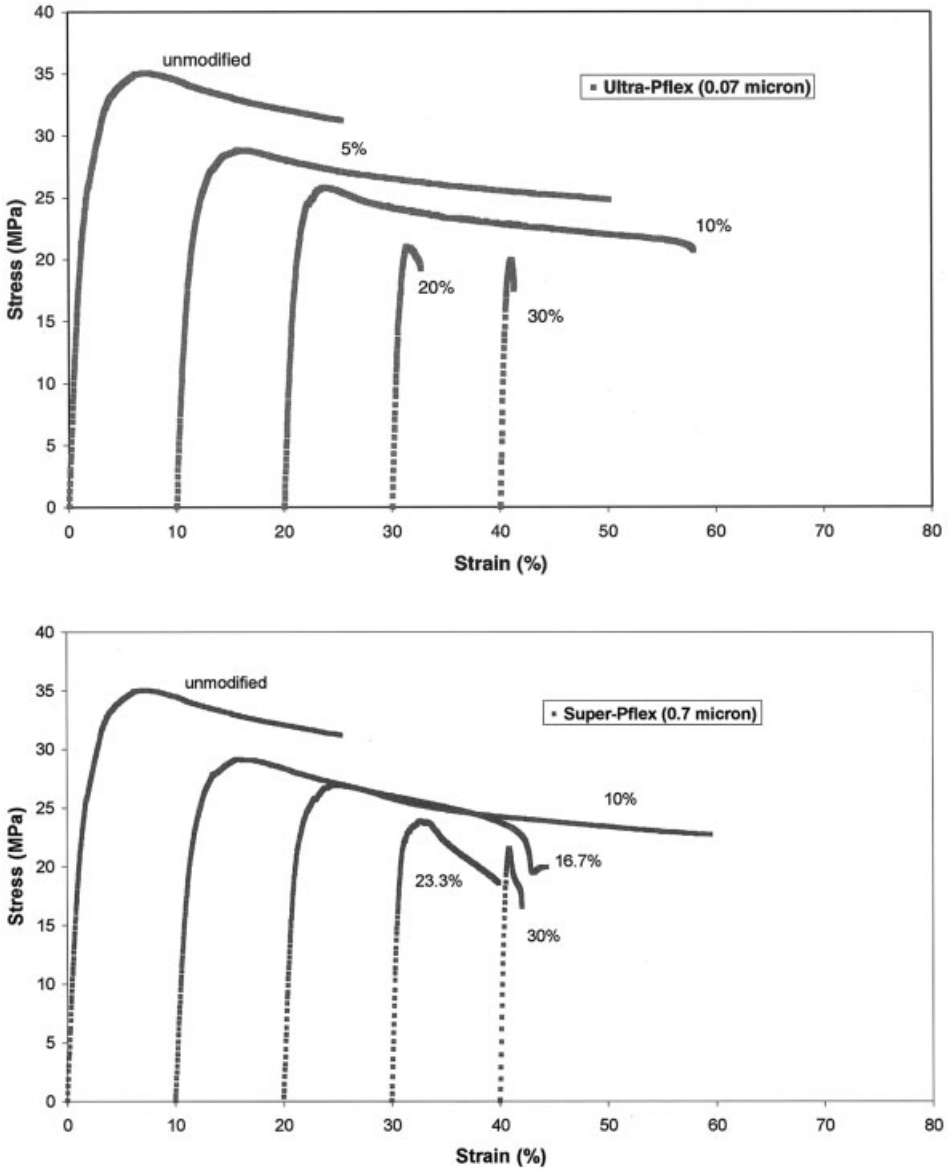

Figure 1 Stress–strain curves for (a) $CaCO_3$ (0.07 μm)/iPP, (b) $CaCO_3$ (0.7 μm)/iPP, and (c) $CaCO_3$ (3.5 μm)/iPP composites.

voids formed at the onset of debonding will produce an observable positive deviation from the unfilled polymer's behavior. This article also discusses how measurement of the evolution of volume at larger strains can provide insight on the microscopic structure of these composites.

EXPERIMENTAL

Sample preparation

Isotactic polypropylene (iPP) Accpro 9346 from BP Amoco Polymers, Inc. was used. The filler particles were calcium carbonate ($CaCO_3$) obtained from Specialty Minerals Inc. Three types of particles were used with average particle size of 0.07, 0.7, and 3.5 μm. They will be referred to as CC0.07, CC0.7, and CC3.5, respectively. The particles have been treated using stearic acid. More details on these particles and sample compounding are given elsewhere.[7] For each type of particle, four volume fractions were used, ranging from 5 to 30%. Dog-bone tensile bars of these composites and of unfilled iPP were molded with nominal gauge length of 50 mm, width of 12.7 mm, and thickness of 3.2 mm (ASTM D638 Type I).

Tensile dilatometry tests

Tensile tests were carried out with an Instron 1430 apparatus, following the ASTM D638 procedure, at a crosshead speed of 10 mm/min, which corresponds to a strain rate of 0.4 min^{-1}. At least three samples of each material were tested at room temperature. The

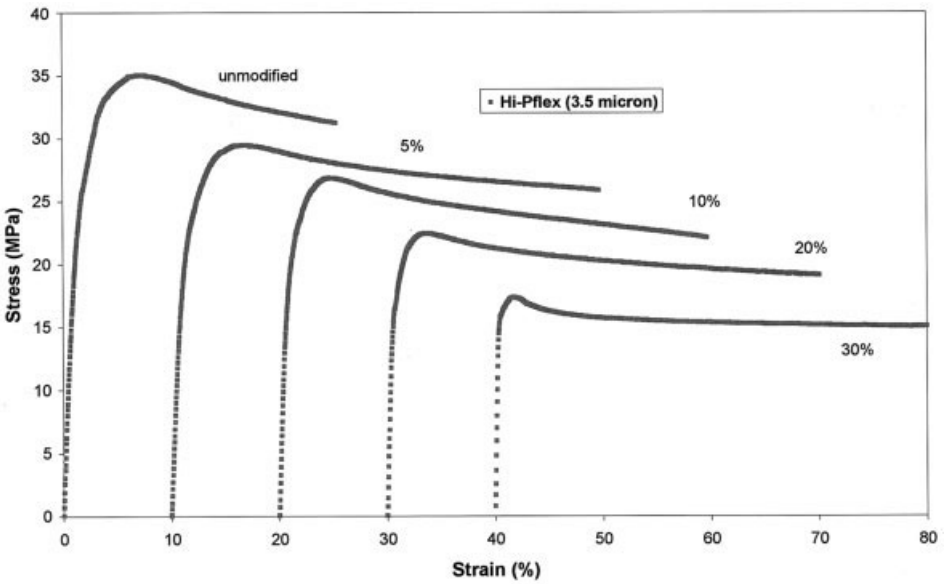

Figure 1 (*Continued from the previous page*)

Instron was connected to a computer for data collection and analysis. Elongation and specimen width were measured during deformation using two extensometers: one along the tensile direction (axial), and the other perpendicular to it (lateral). The two lateral strain components were assumed to be equal. The volume strain is then given by

$$\frac{\Delta V}{V_0} = (1 + \varepsilon_1)(1 + \varepsilon_2)^2 - 1 \qquad (1)$$

where ΔV is the change in volume, V_o the original volume, ε_1 the axial strain, and ε_2 the lateral strain.

RESULTS AND ANALYSIS OF THE EXPERIMENTAL DATA

Stress–strain behavior

The stress–strain curves of the tested materials are given in Figures 1(a)–(c). The addition of $CaCO_3$ increases the modulus and decreases the tensile strength of the composites. At small volume fractions, the particles also increase the elongation at break although further addition of $CaCO_3$ decreases it. This observation has been reported in a previous publication.[7] Slight discrepancies between the values reported therein and those reported here can be attributed to the difference in the methods employed in measuring the axial strain.

Figure 2 presents the dependence of Poisson's ratio, taken as $-\varepsilon_1/\varepsilon_2$ at low ε_1, on the filler volume fraction ϕ. Poisson's ratio is effectively independent of particle size. The small decrease of Poisson's ratio with increasing volume fraction is a result of increasing contribution of the particles, whose Poisson's ratio is lower than that of the matrix.

Onset of debonding

The onset of debonding can be determined from the volume strain measurement at small axial strains. Figure 3 shows an example of how the stress and the strain at the onset of debonding have been calculated. When debonding occurs and voids are formed, the volume of the composites will increase more than the contribution of the matrix alone.

The results are given in Figure 4(a) and (b), where the stress and strain at the onset of debonding are plotted as a function of particle content. Comparison with the values of stress and strain [Fig. 1(a) to (c)] shows that debonding generally occurs before yield-

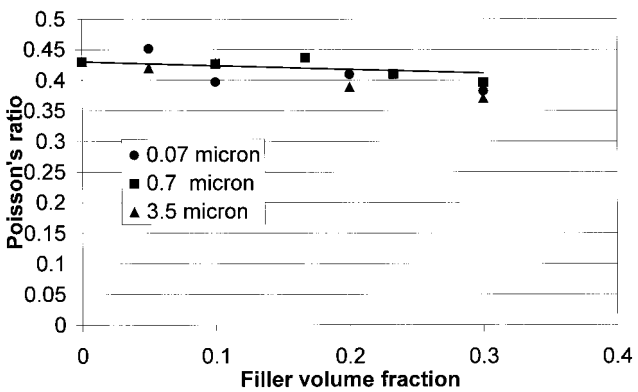

Figure 2 Variation of Poisson's ratio vs particle volume fraction of PP/$CaCO_3$ composites with different filler particle size.

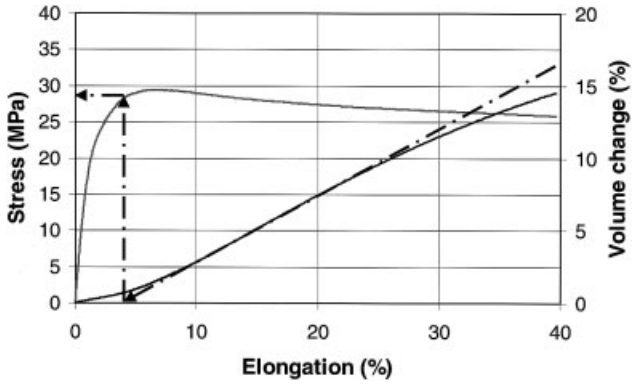

Figure 3 Example of graphical determination of the stress and strain at debonding.

ing, as conjectured from qualitative observation in a previous publication.[7] In fact, a linear correlation between initiation (debonding) stress and yield stress with slope one and zero interception found by Pukánszky et al.[15] does not hold in this case. Particle size does not appear to affect the onset strain at debonding. Consideration of the stress at the onset of debonding reveals that the composites with intermediate particle size (0.7 μm) show a slightly higher resistance to debonding, especially at larger filler loadings. Increasing volume fraction leads to earlier debonding, consistent with the observed reduction in strain at yield as particle content increases. Because the presence of the voids reduces the macroscopic plastic resistance, earlier void formation leads to earlier macroscopic yield.

Volume strain behavior at large axial strains

Figure 5(a)–(c) shows the volume strain evolution as a function of axial strain for the composites at different volume fraction. All materials show a clear increase in volume after yielding. Even the unmodified iPP shows a volume expansion after a small plastic plateau. Because no volume should be generated in the ideal plastic case where only shear deformation occurs, the persistent increase in volume of the unmodified iPP must be due to some form of crazing or microvoiding process. Although the detailed mechanism is still to be clarified, crazing in iPP has been reported.[16–18] The measured value for Poisson's ratio of iPP is 0.43, which compares well with the value of 0.41 reported by Pukánszky et al.[15]

In every composite included in Figure 5(a)–(c), the volume strain past the yield point depends linearly on axial strain. Furthermore, contrasting the data reported by Pukánszky et al.,[15] the variation with volume fraction also suggests linearity, as is better shown in Figure 6(a)–(c).

Farris[19] proposed a correlation for the description of the composition dependence of volume strain in filled elastomers that predicted a linear dependence of volume evolution with axial strain. Lazzeri et al.[20] applied it to $CaCO_3$-filled unplasticized PVC, and later Pukanszky et al.[15] used it for PP filled with $CaCO_3$ of different particle sizes.

Similar to Farris[19] we hypothesize that the strain-induced volume dilatation presented by the materials studied in this work are related to the formation and growth of microvoids following debonding at the filler–matrix interface. Unlike the filled rubbers studied by Farris,[19] solid polymers can also show a strain-induced volume dilatation. For this reason the contribution of the matrix has to be taken into account. The overall strain-induced volume evolution for filled composites can thus be represented with the following equation:

$$\left(\frac{\Delta V}{V_0}\right)_C = \left(\frac{\Delta V}{V_0}\right)_M (1 - \phi) + c\phi\varepsilon_1 \qquad (2)$$

where $(\Delta V/V_0)_c$ is the volume strain of a composite as measured, $(\Delta V/V_0)_M$ the volume strain of the matrix component in the composite, ϕ the filler volume fraction, ε_1 the axial strain, and c a coefficient for the rate

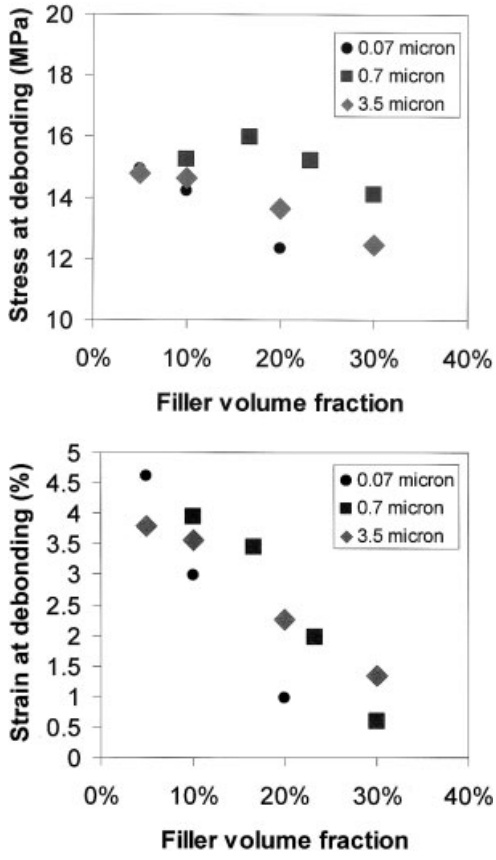

Figure 4 Stress (a) and strain (b) at debonding versus particle volume fraction of PP/$CaCO_3$ composites with different filler particle size.

of volume evolution. $(\Delta V/V_0)_M$ is taken to be a function of strain only; and includes both elastic expansion and volume increases due to other mechanisms (crazing, microvoiding, and structural rearrangements). Furthermore, $(\Delta V/V_0)_M$ is not necessarily the same as the volume strain of the unfilled iPP.

In a set of composites filled with the same particle type and for a given axial strain, there are several experimental values of $(\Delta V/V_0)_c$, each at a particular volume fraction [filled circles in Fig. 6(a)–(c)]. Equation (2) implies that extrapolation of these $(\Delta V/V_0)_c$ value to zero volume fraction gives a value for $(\Delta V/V_0)_M$ at the selected axial strain. These values are the y-axis intercepts of the lines in Figure 6(a)–(c). Therefore, it is possible to construct the volume evolution curve of the matrix component as a function of axial strain. These curves for the three different fillers are reported in Figure 7. The curve for the CC3.5 filler is quite similar to that of the unfilled iPP, while those for CC0.07 and CC0.7 deviate from it significantly. This behavior has not been reported previously, and we offer an initial hypothesis to explain these results. Our observations of the matrix volume evolution suggest that the ligaments of matrix in the composites filled with CC3.5 behave as if the particles were not present. The two smaller particle types impose a smaller characteristic thickness of interparticle ligaments[22] that may hinder the microvoiding or crazing process that is characteristic of the bulk unmodified iPP material.

Once the behavior of the matrix component has been determined, it is useful to rearrange eq. (2) as follows:

$$\frac{\partial}{\partial \varepsilon_1}\left[\left(\frac{\Delta V}{V_0}\right)_C - \left(\frac{\Delta V}{V_0}\right)_M (1-\phi)\right] = c\phi \qquad (3)$$

where the left hand-side can be calculated from experimental data. Calculated values for the left-hand side of the equation are given in Figure 8 as a function of ϕ. The values for each particle type can be fitted well with a line, the slope being c as given in eq. (3). Figure 8 shows that c varies with average particle size D and larger particles exhibit lower values of c. The dependence is in fact quite linear with $1/D$, as is demonstrated in Figure 9. This relationship suggests that the specific surface area of the fillers, proportional to $1/D$, affects the volume evolution. This result is not predicted by the Farris model,[19] which is not particle size dependent.

In a previous study,[21] aggregation was shown to start around 6 m^2/g specific surface area in $CaCO_3$/PP composites when the filler is not coated; aggregation may also play a role in the stearic acid modified materials studied here. Aggregation depends on filler characteristics, composition, surface modification, and processing conditions. In the present context, the inner part of an agglomerated or aggregated particle might not be accessible to the polymer during melt mixing, thus giving rise to an excluded volume effect. This would result in a effective volume fraction larger than the nominal, and therefore, the presence of agglomerates and aggregates might give rise to a larger volume strain compared to that predicted by eq. (2).

In the case of the materials studied in this work all particles were coated with stearic acid, thus minimizing the tendency for aggregation, as confirmed by SEM analysis. The limited role of size-dependent aggregation on the observed volume change in the composites studied here is analyzed in detail below. We postulate instead that the dominant cause for the unanticipated particle size dependence shown in Figure 9 is a particle–matrix interphase that affects the deformation behavior of the composite material. Composites containing rigid particles can be viewed as composed of three phases: the particle, the matrix, and an interphase layer. Others have shown[9] that such an interphase layer, consisting of short chains of the matrix polymer and any surface modifier on the particles, can be immobilized on the surface of the particles. The particles used in this study were treated using stearic acid, which intermixes with or interpenetrates the iPP chains near the surface of the particles creating an interphase layer. If this immobilized layer is present in the systems studied here, debonding will occur not directly at the particle surface but at a weaker interface between the immobilized layer and the matrix. This phenomenon is depicted in Figure 10. The overall effect, in terms of volume evolution, is to increase the effective volume fraction of the particles due to the addition of the immobilized layer. Because only the nominal volume fraction (calculated on the basis of filler and matrix density) has been used in the analysis above, a correction term must be introduced into eqs. (2) and (3).

A first-order model can be developed to calculate the correction term for the effective volume fraction. A cubic representative volume element with size L contains a particle of diameter D with an interphase layer of thickness δ, as shown in Figure 10. Assuming a small value of δ, the effective volume fraction ϕ_e can be approximated in terms of the nominal volume fraction ϕ:

$$\phi_e = \frac{\pi D^3/6 + \pi D^2 \delta}{L^3} = \phi\left(1 + \frac{6\delta}{D}\right) \qquad (4)$$

Rewriting eq. (3) using the effective volume fraction instead of the nominal:

$$\frac{\partial}{\partial \varepsilon_1}\left[\left(\frac{\Delta V}{V_0}\right)_C - \left(\frac{\Delta V}{V_0}\right)_M \left[1 - \phi\left(1 + \frac{6\delta}{D}\right)\right]\right] = k\phi\left(1 + \frac{6\delta}{D}\right) \qquad (5)$$

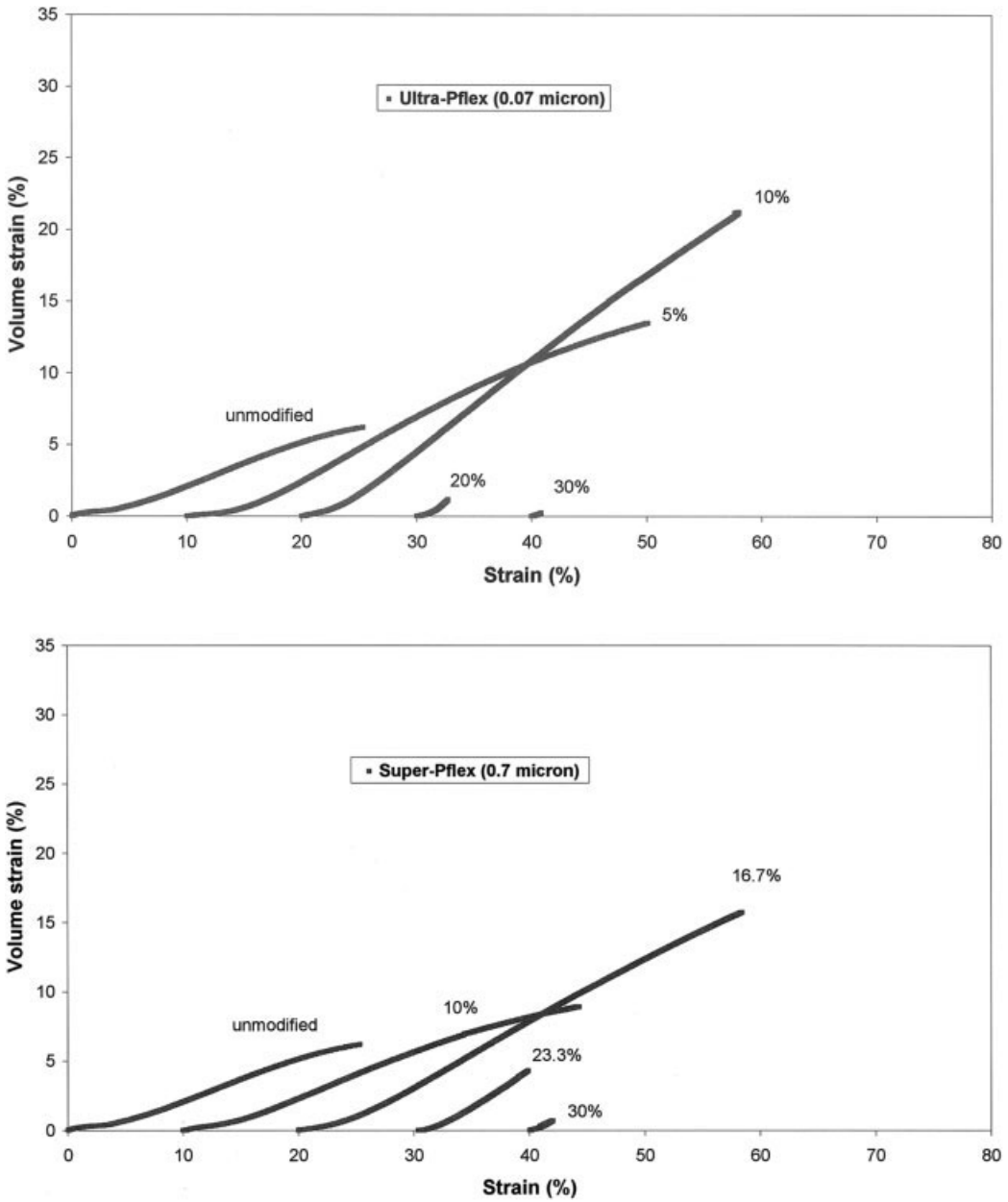

Figure 5 Volume strain–elongation curves for (a) $CaCO_3$ (0.07 μm)/iPP, (b) $CaCO_3$ (0.7 μm)/iPP, and (c) $CaCO_3$ (3.5 μm)/iPP composites.

where the coefficient k is now used to distinguish it from c used in eq. (3). The unknowns k and δ can be calculated through best fit of the data, analogous to the calculation done above to obtain c. The resulting values are $k = 1.65$ and $\delta = 25$ nm. The value of k is expected to be 1, as suggested by Farris,[19] in the ideal case of linear elongation of the void with increasing axial strain; a value of 1.65 indicates some deviation from the elongated-ellipse shape. A thickness of the interphase layer of 25 nm is consistent with several other works on filled iPP systems employing different experimental techniques[23–25] that reported values of interphase layer thickness ranging from 1 to 160 nm.

DISCUSSION

The results reported in the present article show that particle debonding, void growth, and plastic stretch of the interparticle ligaments, observed in SEM analysis on the same set of materials,[7] gives rise to a measurable volume change during tensile test. In the previous publication, several differences were noted about the types of filler used.[7] The size distribution of CC3.5 was quite broad while, due to the different production route used, that of the precipitated particles was narrower. Moreover, the spatial dispersion was relatively good for the two larger particle sizes at filler volume

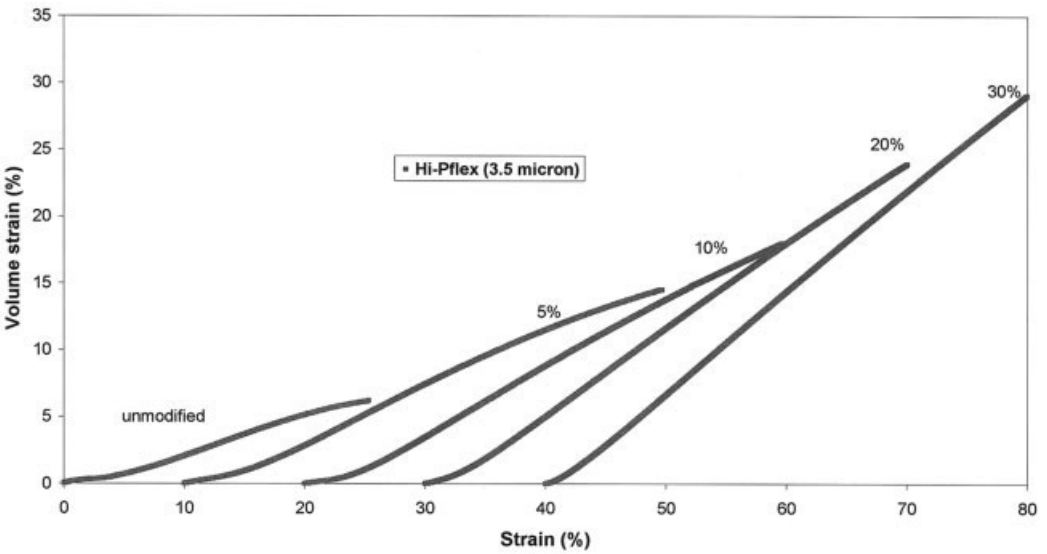

Figure 5 (*Continued from the previous page*)

fractions below 20%, above which large agglomerates were observed, with sizes in the range of 10–100 times the nominal average particle diameter. For the blends with CC0.07, a strong tendency to agglomerate was observed even at low volume fractions. This effect might be related to the different surface concentration of the stearate molecules on the three powders.

The data reported in this work show a clear particle size effect on volume change, which was not seen in the work of Pukánszky et al.[15] These authors used four different types of uncoated particles with average size 58, 3.6, 3.6, and 1.3 μm and a correspondent specific surface of 0.5, 2.2, 3.3, and 5 m^2/g. Our volume strain data for pure iPP and that filled with 30 vol % $CaCO_3$ with 3.5-μm size are almost identical to those reported in Figure 4 of ref. 15. In our study we examined stearic acid coated particles and, significantly, we also used two smaller particle sizes, 0.07 and 0.7 μm.

In the previous section we noted that the presence of significant amounts of large agglomerates might affect the volume strain data. One aspect that appears especially critical is how much polymer or even air is entrapped in the large agglomerates. During tensile deformation, an agglomerate tends to behave as a single large particle.[7] The polymer or the air entrapped in such an agglomerate will raise the effective filler content and alter the calculation made using the model proposed above. In particular, the thickness of the immobilized layer δ would be affected.

To thoroughly address this point and, in particular, to evaluate the effect of excluded volume on the effective filler volume fraction, a simple model was developed and is presented in Appendix A. By using a value of the agglomerate packing density η in the range 0.3–0.5[26] and the data on the fraction of agglomerated particles, reported in Table I and calculated from the SEM analysis carried out in a previous study of the very same series of materials,[7] we obtain values of δ in the interval 13–19 nm and k between 1.65 and 1.70. Thus, quantitatively and systematically accounting for the presence of agglomerates somewhat alters the calculated value of δ but does not eliminate the strong particle size dependence of the volume strain data that supports the view of the presence of such an interphase layer.

The properties of this interphase are expected to differ significantly from those of the matrix. For some systems, like high-density polyethylene (HDPE) filled with $CaCO_3$ particles covered with stearic acid, a special crystallographic orientation has been shown to be present due to a preferential organization of the crystallites near the filler surface.[10] Although the organic tail of stearic acid can be seen as a short segment of HDPE, it is less similar to iPP, the polymer used in the present work. The stearic acid-rich interphase should interfere with the crystallization of iPP instead of inducing preferential crystallization as in the case of HDPE. Thus, the interphase between iPP and stearic acid-coated $CaCO_3$ particles is more similar in properties to a rubber-like blend of polyethylene and amorphous polypropylene. This hypothesis is also supported by findings by Darlington and Hutley,[27] who reported that, in iPP composites, stearic acid reduces the onset temperature of crystallization and the glass transition temperature of the polymer.[28] Because adhesion between the rubber-like interphase and iPP crystallites is expected to be weak, debonding is likely to occur not at the surface of the $CaCO_3$ particle but at the boundary between the stearate-rich interphase and the bulk iPP matrix. This picture is consistent with the predicted value of 5–20 nm for the thickness of the

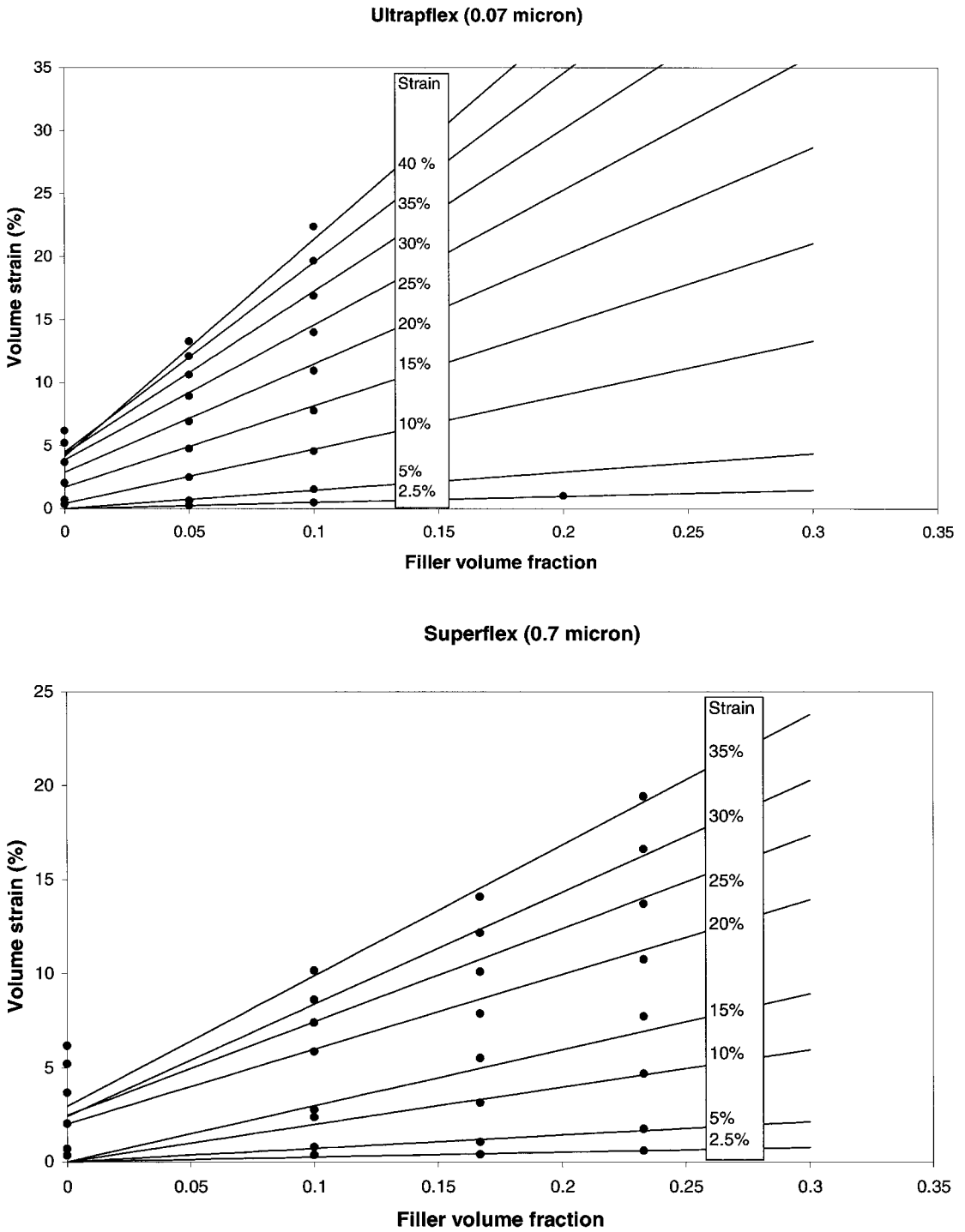

Figure 6 Volume strain vs filler volume fraction at different levels of deformation for (a) $CaCO_3$ (0.07 μm)/iPP, (b) $CaCO_3$ (0.7 μm)/iPP, and (c) $CaCO_3$ (3.5 μm)/iPP composites.

interphase, which is much larger than the fully extended length of the stearic acid tail itself.

An important question is how the volume strain evolution is related to the fracture behavior discussed in a previous publication.[7] That article reported that the only blend exhibiting enhanced impact toughness were CC0.7 compounds at high filler content (>20 vol %). Both the larger (CC3.5) and the smaller (CC0.07) particle types had a detrimental effect on fracture toughness due to the presence of large individual particles and agglomerates, which act as stress-concentrating defects that trigger brittle fracture.

The toughening effect in the CC0.7 composites was shown to be the result of particle–matrix debonding

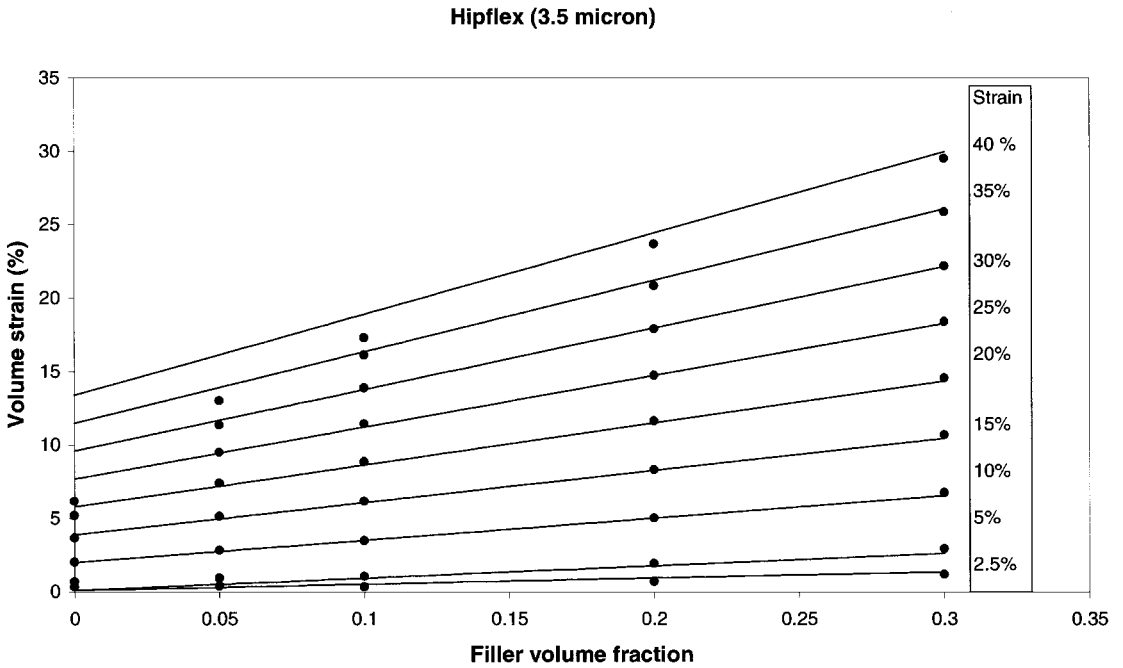

Figure 6 (*Continued from the previous page*)

and plastic stretch of the interparticle ligaments, precisely the phenomena studied here in the volume strain evolution. However, *J*-integral studies showed clearly that the fracture resistance decreases progressively with filler volume fraction, due to the continual reduction in the amount of matrix polymer, the component that actually contributes to energy adsorption.[7] We have shown in the present work that the presence of an interphase layer reduces the effective volume fraction of the deformable matrix. Composites made with smaller particles would exhibit a larger reduction in the amount of deformable matrix because, at a given nominal filler content, the interfacial area between filler and polymer is larger for smaller filler particles. This would cause the composites made with CC0.07 to exhibit lower fracture resistance than those made with larger particles, regardless of the presence of the agglomerates. This effect will, of course, depend on the chemistry of the filler–matrix interface, which determines the thickness and the mobility of the interphase layer.

With this idea, the relationship between the toughness of composites and the particle size becomes a competition of two effects: (1) a detrimental stress-concentrating effect of the particles that becomes more prominent with larger particles and agglomerates, (2) a reduction in the amount of deformable polymer matrix that dominates in composites with smaller par-

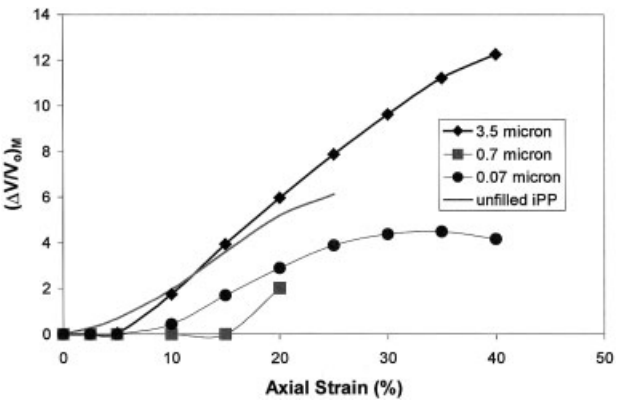

Figure 7 Comparison of experimental and extrapolated volume strain curve for pure iPP matrix. The continuous line refers to the experimental curve while the curves with line and symbols refer to the extrapolated data. See text for details and see graph for meaning of symbols.

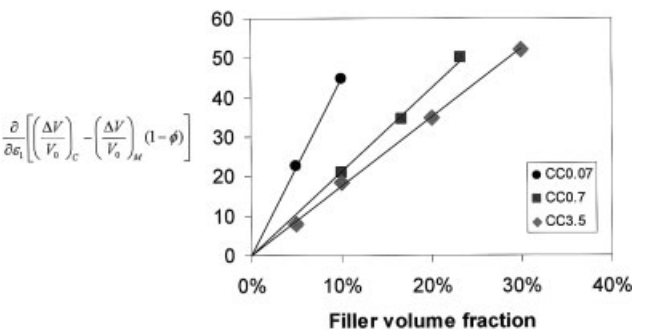

Figure 8 Derivative of $\left[\left(\frac{\Delta V}{V_0}\right)_C - \left(\frac{\Delta V}{V_0}\right)_M (1 - \phi)\right]$ with respect to ε_1 plotted against filler volume fraction at different particle sizes.

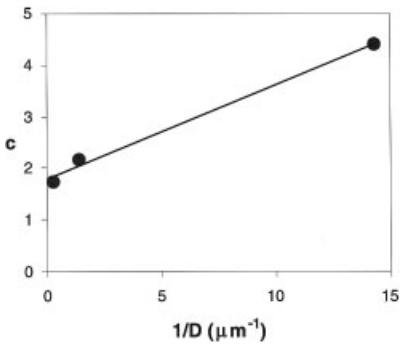

Figure 9 Volume strain coefficient, *c*, vs reciprocal of particle diameter.

ticles. Testing this second effect independently from the first is not straightforward because of the difficulty of eliminating large agglomerates during processing, especially with the smaller particle sizes. This activity is currently in progress and the results will be reported in the future.

CONCLUSIONS

Tensile dilatometry tests on iPP/$CaCO_3$ systems were performed to study the debonding process and the volume evolution of voids inside particulate-filled composites. In the system studied, debonding occurred over a range of stresses but before macroscopic yield, therefore reducing the plastic resistance of the materials. The onset of debonding occurred earlier as particle content increased. Pure iPP shows some volume increase after yielding, indicating a crazing/microvoiding process. All composites also showed significant amounts of increase after yielding, associated with the growth of voids nucleated around the particles. The volume growth was a linear function of particle volume fraction and axial strain; the smallest particles showed the highest rate of volume increase.

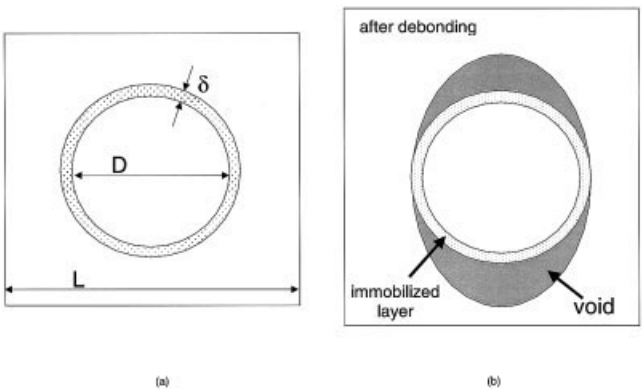

Figure 10 (a) Model for effective filler volume fraction calculation. (b) Model for volume increase due to debonding and cavity growth.

TABLE I
Effect of Aggregation on Effective Filler Volume Fraction

Nominal volume fraction, ϕ_N	Effective volume fraction, ϕ^E		
	$\eta = 0.3$	$\eta = 0.5$	α
HiPflex 3.5 micron			
0	0	0	0
0.05	0.050	0.050	0.001
0.10	/	/	/
0.20	/	/	/
0.30	0.369	0.329	0.098
SuperPflex 0.7 micron			
0	0	0	0
0.10	0.108	0.104	0.035
0.167	/	/	/
0.233	/	/	/
0.30	0.359	0.325	0.084
UltraPflex 0.07 micron			
0	0	0	0
0.05	0.057	0.053	0.063
0.10	0.142	0.118	0.180
0.20	0.376	0.275	0.377
0.30	0.599	0.428	0.427

A simple model was proposed to account for the observed particle-size dependence. The model includes an interphase layer between particle and matrix, the thickness of which was estimated from the data to be about 15–25 nm. The role of aggregates has been considered, and their presence, in the amounts quantified in earlier work on the very same compounds, has negligible effect on the observed values of volume strain in our experiments.

The measurement of volume evolution as a means for characterizing the interphase layer is a relatively simple but powerful method. Careful measurements of volume dilation can facilitate more complete understanding of microstructure in rigid-particle–filled polymer systems and provide insights into the design of thermoplastic polymer composites with improved stiffness and toughness.

We thank Dr. Mark Weinberg of E.I. duPont de Nemours Co. for his help in preparing the samples.

APPENDIX A

The basic assumptions of the model described in this appendix are that agglomerates are difficult for the molten polymer to be fully infiltrated during extrusion and injection molding, leaving the core of the agglomerate impermeable, giving rise to an excluded volume effect.[26] This results in an effective volume fraction of the agglomerates being larger than that can be calculated on the basis of the densities of the matrix and of the filler. The effective degree of polymer saturation of the pores present in an aggregate varies with mor-

phology and surface treatment of the particles, matrix viscosity, and chemistry and the presence of air.[26] The model assumes that all aggregates do contribute to the volume evolution behaving as very large effective single particles that debond, remaining in one piece, or a large particle that cavitates/fractures internally. The reality can be different, because SEM analysis has shown that not all the aggregates and agglomerates debond and fracture.[7] Also, the model does not make any distinction between agglomerates—which tend to be very large with loosely bonded particles—and aggregates—formed by a few tightly bonded particles. The amount of excluded volume is predictably larger for agglomerates than for aggregates. To obtain an upper bound estimate of the effects of agglomerates and aggregates in the model no distinction has been made between these two types of collection of particles.

We assume that the total nominal volume fraction is ϕ_N. The nominal volume fraction of agglomerated particle is $\phi_1 = \alpha\ \phi_N$, while the volume fraction of nonagglomerated particles is:

$$\phi_2 = (1 - \alpha)\phi_N$$

The effective volume fraction of the agglomerated particles is

$$\phi_1^E = \frac{\phi_1}{\eta} = \frac{\alpha\phi_N}{\eta}$$

where η is the packing factor.

The total effective volume fraction is then:

$$\phi_T^E = \frac{\phi_1}{\eta} + \phi_2 = \frac{\alpha\phi_N}{\eta} + (1 - \alpha)\phi_N = \left[\frac{\alpha}{\eta} + (1 - \alpha)\right]\phi_N \quad \text{(A1)}$$

In Table I are reported the values of the effective filler volume fraction ϕ^E for the different materials studied in this work calculated according to eq. (A1). The values of the fraction of agglomerated particles, α, is calculated from SEM analysis of the fracture surface carried out in a previous article on the same set of materials.[7] The data reported in Table I are calculated for two values of the packing factor η, which represents the typical extremes for agglomerated $CaCO_3$ particles.[26]

References

1. Lazzeri, A.; Bucknall, C. B. J Mater Sci 1993, 28, 6799.
2. Lazzeri, A.; Bucknall, C. B. Polymer 1995, 36, 2895.
3. Lazzeri, A.; Bucknall, C. B. In Toughening of Plastics; Pearson, R. A.; Sue, H. J.; Yee, A. F., Eds.; ACS Symp No. 759; Oxford University Press: London, 2000, p. 14.
4. Levita, G.; Marchetti, A.; Lazzeri, A. Polym Comp 1989, 10, 39.
5. Demjen, Z.; Pukanszky, B.; Nagy, J. Compos Part A 1998, 29, 323.
6. Jancar, J.; Dibenedetto, A. T. Polym Eng Sci 1993, 33, 559.
7. Thio, Y. S.; Argon, A. S.; Cohen, R. E.; Weinberg, M. Polymer 2002, 43, 3661.
8. Kim, G. M.; Michler, G. H. Polymer 1998, 39, 5689, 5699.
9. Pukánszky, B.; Fekete, E. In Mineral Fillers in Thermoplastics I. Raw Materials and Processing; Advances in Polymer Science; Jancar, J., Ed.; Springer-Verlag, Berlin, 1999, p. 109, vol. 139.
10. Argon, A. S.; Bartczak, Z.; Cohen, R. E.; Muratoglu, O. K. In Pearson, R. A.; Sue, H. J.; Yee, A. F., Eds.; Toughening of Plastics; ACS Symp No. 759; Oxford University Press, London, 2000, p. 98.
11. Wilbrink, M. W. L.; Argon, A. S.; Cohen, R. E.; Weinberg, M. Polymer 2001, 42, 10155.
12. Kraus, R.; Wilke, W.; Zhuk, A.; Luzinov, I.; Minko, S.; Voronov, A. J Mater Sci 1997 32, 4397.
13. Miller, A. C.; Minko, S.; Berg, J. C. J Adhesion 2001, 75, 257.
14. Bucknall, C. B. Toughened Plastics; Applied Science: London, 1977.
15. Pukánszky, B.; Van es, M.; Maurer, F. H. J. J Mater Sci 1994, 29, 2350.
16. Jang, B. Z.; Uhlmann, D. R.; Vander Sande, J. B. Polym Eng Sci 1985, 25, 98.
17. Narisawa, I.; Ishikawa, M. In Crazing in Polymers, Kausch, H. H., Ed.; vol. 2. Advances in Polymer Science; Springer-Verlag, Berlin, 1990, 0. 354, vol. 91/92.
18. Huetink, J.; Van Dijk, D. J.; Dijkstra, P. T. S. Polym Eng Sci 2002, 42, 152.
19. Farris, R. J. Trans Soc Rheol 1968, 12, 315.
20. Lazzeri, A.; Levita, G.; Marchetti, A. Proc. 1st International Conference on "Deformation, Yield and Fracture of Composites" at UMIST, Manchester, UK, 25–27 March 1991, p. 28/1.
21. Pukánszky, B.; Fekete, E. Polym Polym Comp 1998, 6, 313.
22. Wu, S. J Appl Polym Sci 1988, 35, 549.
23. Akay, G. Polym Eng Sci 1990, 30, 1361.
24. Mansfield, K. F.; Theodorou, D. N. Macromolecules 1991, 24, 4295.
25. Pukanszky, B.; Tudos, F. In Controlled Interphases in Composite Materials; Ishida, H., Ed.; Elsevier: New York, 1990, p. 691.
26. Levresse, P.; Manas-Zloczower, I.; Feke, D. L.; Bomal, Y.; Bortzmeyer, D. Powder Technol 1999, 106, 62.
27. Darlington, M. W.; Hutley, T. E. Polym Commun 1985, 26, 264.
28. Darlington, M. W. BPF/Brunel University Conf. Filled Plastics, Filplas '81, September 1981.